Hydrogen Bond Dissociation and Reformation in Methanol Oligomers Following Hydroxyl Stretch Relaxation

K. J. Gaffney, Paul H. Davis,† I. R. Piletic, Nancy E. Levinger,‡ and M. D. Fayer*

Department of Chemistry, Stanford University, Stanford, California 94305

Received: July 22, 2002; In Final Form: October 2, 2002

Vibrational relaxation and hydrogen bond dynamics in methanol-*d* dissolved in CCl_4 have been measured with ultrafast infrared pump−probe spectroscopy. We excited the subensemble of methanol-*d* molecules both accepting and donating hydrogen bonds at ∼2500 cm^{-1}. Following vibrational relaxation with a ∼500 fs lifetime, the signal does not decay to zero. Rather, the signal increases to a second maximum at ∼4 ps. The decay from the second maximum occurs on two time scales. We propose a model in which hydrogen bond dissociation, following vibrational relaxation, decreases the concentration of methanol-*d* molecules that accept and donate hydrogen bonds and produce the observed long-lived bleach of the absorption signal. Using a set of coupled kinetic equations, the time constants for hydrogen bond dissociation and reformation have been determined. Hydrogen bond breaking occurs with ∼200 fs and ∼2 ps time constants. We attribute the fast rate to a direct breaking mechanism wherein the excited hydroxyl stretch decays into modes that directly lead to the hydrogen bond dissociation. The slower rate of breaking is attributed to an indirect mechanism wherein the dissociation of hydrogen bonds follows vibrational energy flow from the initially excited molecule to other components of the same oligomer. The final stage of relaxation, after the second maximum, involves reformation of transiently broken hydrogen bonds. The bonds that break directly recover with ∼7 ps and ≫10 ns time constants, while the bonds that break indirectly recover with ∼20 ps and ≫10 ns time constants. Experiments conducted on ethanol-*d* solutions in CCl_4 demonstrate that the same vibrational relaxation and hydrogen bond dynamic events occur with very similar amplitudes and rate constants. Measurements of the rates of spectral diffusion and polarization anisotropy decay via vibrational excitation transfer and orientational relaxation verify that the initial fast decay of the signal is dominated by vibrational relaxation.

I. Introduction

The vast majority of chemistry and biology occurs in hydrogen-bonding liquids, such as water and alcohols. For a chemical transformation to occur in solution, the solvent must stabilize the reaction products. The solvent is an active partner in the reaction, structurally reorganizing to stabilize the products and serving as an energy source or sink. The dynamic properties of a particular solvent can enhance or hinder the rate and yield of a chemical reaction relative to reaction in another solvent.[1−6] For hydrogen-bonding solvents, the structural evolution of extended hydrogen-bonding networks is a key factor in determining the solvent's overall dynamics and the rate of intermolecular energy flow.[7,8]

This paper presents the results of time and spectrally resolved ultrafast infrared vibrational pump−probe experiments on the dynamics of hydrogen bond dissociation and reformation in methanol-*d* clusters dissolved in carbon tetrachloride. Analysis of the linear infrared absorption spectrum provides essential information for the interpretation of the time-resolved data.[9−13] The formation of hydrogen bonds substantially influences the frequency and width of the hydroxyl stretch vibration of methanol.[8] For a low concentration of methanol-*d*, a relatively narrow monomer peak appears at ∼2690 cm^{-1} with a ∼20 cm^{-1} full width at half-maximum (fwhm), as shown in Figure 1.[9−13] As the concentration increases, methanol forms hydrogen-bonded oligomers.[10,11,13−15] Open chain oligomers have two terminal molecules spectroscopically distinct from the internal methanol-*d* molecules, as well as each other. The terminal β methanol that accepts but does not donate a hydrogen bond has a transition frequency and width indistinguishable from the monomer.[11−13] The terminal γ methanol that donates but does not accept a hydrogen bond has a transition frequency of ∼2600 cm^{-1} and an ∼80 cm^{-1} fwhm.[10−13] The internal δ methanol-*d* molecules that accept and donate hydrogen bonds have a maximum transition frequency at ∼2490 cm^{-1} and a ∼150 cm^{-1} fwhm.[10,11,13] The spectroscopic data demonstrate that the formation of hydrogen bonds shifts the frequency of the hydroxyl stretch and broadens the absorption. As the methanol-*d* concentration increases, the amplitudes of the β and γ peaks decrease while the δ peak increases. By 26 mol %, the β peak has a very small amplitude and the γ cannot be distinguished from the δ absorption.

The vibrational dynamics of δ absorbers have been widely investigated with infrared pump−probe spectroscopy, particularly for ethanol dissolved in CCl_4.[9,16−23] Despite the wide range of studies, the majority have lacked sufficient time resolution and sufficient sensitivity to unambiguously observe the initial stages of the hydroxyl stretch relaxation. The investigation of ethanol-*h* dissolved in CCl_4 conducted by Woutersen et al.[23] and methanol-*h* dissolved in CCl_4 conducted by Laenen et al.[21] provides notable exceptions. Woutersen et al. found the ethanol

* To whom correspondence should be addressed.
† Current address: Department of Chemistry, Santa Clara University, Santa Clara, CA 95053.
‡ On sabbatical leave from the Department of Chemistry, Colorado State University, Fort Collins, CO 80523.

10.1021/jp021696g CCC: $22.00
Published on Web 11/23/2002

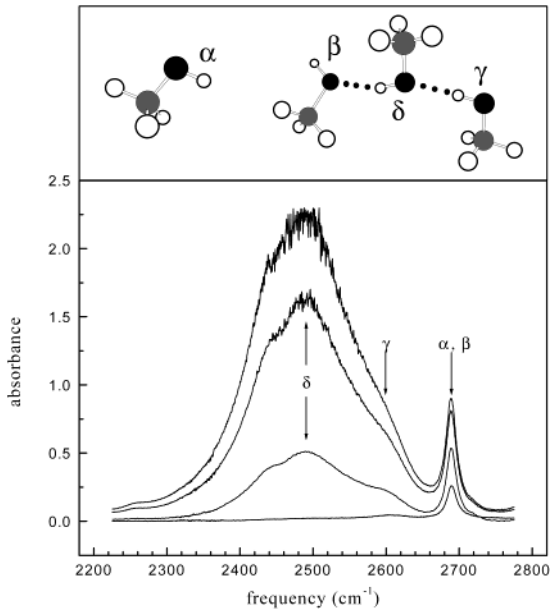

Figure 1. Steady state IR spectrum of methanol-*d* in CCl_4 as a function of concentration in mole percent. Concentrations of 1.0, 2.5, 3.8, and 5 mol % appear from bottom to top. α refers to isolated monomeric molecules, β refers to ODs that accept but do not donate hydrogen bonds, γ refers to molecules that donate but do not accept hydrogen bonds, and δ refers to molecules that donate and accept hydrogen bonds. The drawing of a monomer and a trimer shows the different types of hydroxyl groups with the appropriate labels.

OH stretch excited state lifetime to range from 250 fs when exciting and probing at the 3330 cm^{-1} absorption maximum to 900 fs at a laser frequency of 120 cm^{-1} to the blue of the maximum. Laenen et al. found the methanol OH stretch lifetime to range from 450 ± 50 to 600 ± 50 fs as the excitation frequency of the laser shifted from 3280 to 3400 cm^{-1} about the absorption maximum at ∼3330 cm^{-1}. In addition to the initial excited state relaxation, both studies observed the dissociation of hydrogen bonds following vibrational excitation.

While both studies conclude that hydroxyl stretch relaxation leads to hydrogen bond breaking, how vibrational relaxation leads to hydrogen bond dissociation remains unclear. Woutersen et al. argue that the excited OH stretch of ethanol decays directly to hydrogen bond continuum states above the hydrogen bond dissociation threshold.[16,23,24] Within this model of direct relaxation of the excitation energy to the hydrogen-bonding coordinate, vibrational relaxation and hydrogen bond dissociation occur simultaneously. The broken hydrogen bonds in the ethanol oligomers subsequently reform with a 15 ps time constant. In contrast, Laenen et al. observe a rise in the pump−probe signal to the red of the OH stretch absorption maximum following vibrational relaxation, suggesting the delayed dissociation of hydrogen bonds following vibrational relaxation.

The direct dissociation mechanism cannot explain hydrogen bond dissociation for alcohols that do not donate a hydrogen bond, making β absorbers ideal for investigating the dynamics of sequential hydrogen bond dissociation. We have reported hydrogen bond dissociation dynamics for methanol-*d*, ethanol-*d*, and *n*-propanol-*d*.[25,26] For all three alcohols, relatively fast and efficient hydrogen bond dissociation follows the vibrational relaxation of β absorbers. For 5 mol % methanol-*d*, hydrogen bond breaking occurs with a time constant of 2.5 ± 1 ps, with hydrogen bond dissociation occurring for roughly one in three excited β methanol-*d* molecules. While this clearly establishes the significance of sequential hydrogen bond dissociation mechanisms for molecules that accept but do not donate hydrogen bonds, the relative importance of simultaneous and sequential hydrogen bond dissociation mechanisms has yet to be determined for alcohols that both donate and accept hydrogen bonds. With this objective in mind, we report here on a series of experiments that have been conducted on δ methanol-*d* dissolved in CCl_4 excited near the peak of the δ band at ∼2500 cm^{-1} and the subsequent relaxation of the excited state populations. The results show that vibrational relaxation occurs with a ∼500 fs time constant. Hydrogen bond dissociation takes place after vibrational relaxation on two time scales, ∼200 fs and 2 ps. Studies of vibrational relaxation and hydrogen bond breaking and reformation have also been conducted on ethanol-*d* in CCl_4. These experiments demonstrate that all stages of the relaxation occur with rate constants very similar to those found for methanol-*d* solutions. Measurements of spectral diffusion using frequency-resolved pump−probe experiments and measurements of orientational relaxation and vibrational excitation transfer using polarization selective pump−probe experiments show that while all three of these phenomena happen, their rates are slower than the initial vibrational relaxation and the fast hydrogen bond breaking.

II. Experimental Methodology

Deuterated methanol-*d* (Aldrich, 99.5+ atom %), protonated methanol-*h* (J. T. Baker, spectroscopic grade), deuterated ethanol-*d* (Aldrich, 99.5+ atom %), and carbon tetrachloride (Aldrich, HPLC grade) were used as received. Methanol-*d* and ethanol-*d* have deuterated hydroxyl groups and protonated methyl groups. Samples were prepared by weight at 2.5, 5, and 26 mol % for methanol-*d* in CCl_4. An additional sample of 0.8 mol % methanol-*d*/23 mol % methanol-*h* in CCl_4 was prepared. Spectroscopic measurements used home-built copper cells with CaF_2 windows. Teflon spacers from 50 μm to 1 mm yielded absorbances in the range of 0.5−1.2, respectively, for the δ peak at ∼2500 cm^{-1} for all solutions studied. In these sample cells, the solution came in contact only with the CaF_2 and Teflon because metals, such as copper, catalyze the decomposition of alcohols in CCl_4 solution.[27]

The laser system used in these experiments consisted of a home-built Ti:Sapphire oscillator and regenerative amplifier whose output pumps a three stage optical parametric amplifier designed and built in-house to produce tunable midinfrared light with controlled pulse duration (spectral bandwidth). A bandwidth limiting slit in the stretcher determined the bandwidth of the amplified seed pulse and provided control of the IR pulse duration. The IR output was 1−2 μJ per pulse centered at ∼2500 cm^{-1}. The IR pulse duration was measured by autocorrelation. The pulses had Gaussian profiles in time and frequency with fwhm of 200 fs in time and 85 cm^{-1} in frequency. The time bandwidth product was always between 1 and 1.25 times the transform limit of 0.44.

The mid-IR pulses were split into pump (90%) and probe (10%) beams that traverse different paths before crossing in the sample. The pump beam was chopped at 500 Hz and directed along a variable path length delay line. A ZnSe Brewster plate polarizer was used to set the probe beam polarization. A small amount of the mid-IR light was split off and used for shot-to-shot normalization. For the frequency-integrated data, signal and reference beams impinged on liquid nitrogen-cooled MCT detectors whose outputs were processed by gated integrators, divided by an analogue processor and input to a lock-in amplifier. A computer controlled a stepper motor delay line and collected the output of the lock-in with an A/D board.

In the frequency-resolved pump−probe experiments, the probe beam was dispersed in a monochromator set to a ∼3 cm^{-1} resolution. By varying the frequency of the monochromator and the time delay between the pump and the probe pulses, the time evolution of the pump−probe signal could be monitored as a function of frequency with high spectral resolution. The frequency-resolved data used an InSb detector and the same reference detector as that used in the frequency-integrated setup. The frequency-resolved data utilized the same data processing electronics and procedures as that of the frequency-integrated data. Frequency-resolved data were collected in two ways. In one, the delay was set and the monochromator was scanned to measure the signal spectrum. This was repeated for a number of delays. Alternatively, the monochromator was set to a particular wavelength, and the delay was scanned. This was repeated for a number of frequencies.

III. Vibrational Relaxation and Hydrogen Bond Dynamics

The initial decay of the pump−probe signal for all concentrations of methanol-*d* in CCl_4 sufficiently high to form oligomers occurs on a subpicosecond time scale, as seen previously for protonated methanol and ethanol. Woutersen et al.[23] and Laenen et al.[21] associated this fast decay with vibrational relaxation. It has also been suggested that vibrational excitation transfer occurs on a subpicosecond time scale.[23] The relative contributions of vibrational relaxation, spectral diffusion, molecular reorientation, and excitation transfer on the initial relaxation must be clarified to accurately determine the dynamics of hydrogen bond dissociation and recombination for methanol oligomers dissolved in CCl_4. A series of experiments have determined the time scales of vibrational excitation transfer, molecular reorientation, and spectral diffusion. In an attempt to limit the length of this paper, the discussion of polarization anisotropy relaxation and spectral diffusion will be limited to their influence on the initial relaxation dynamics. A more thorough analysis of the polarization anisotropy dynamics and spectral diffusion will be reserved for later papers.[28,29] In the following, we first describe the pump−probe dynamics in detail, emphasizing the multiple steps and time scales for hydrogen bond dissociation and reformation following vibration relaxation for methanol dissolved in CCl_4. After we discuss the vibrational relaxation and hydrogen bond dynamics, the role of vibrational excitation transfer, molecular reorientation, and spectral diffusion will be discussed. These affects are readily observed, but they do not strongly influence the vibrational relaxation/hydrogen bond dynamics data analysis.

A. Experimental Results. Figures 2 and 3 display pump−probe data taken on 2.5, 5, and 26 mol % methanol-*d* in CCl_4. Figure 2 shows data taken to 13 ps, while Figure 3 shows the data taken out to 130 ps with reduced point density. The signal decays from its maximum with a time constant of ∼400 fs. It falls to a minimum and then increases to a second maximum at ∼4 ps. The signal then decays on two time scales, one of ∼15 ps and one that is very long, ≫10 ns. The slowly decaying component appears in Figure 3 as a horizontal line offset from zero. Vibrational relaxation of the initially excited OD stretch dominates the initial relaxation, as will be shown in Section IV. We attribute the secondary rise in the signals appearing in Figures 2 and 3, as well as the vibrational relaxation to a nonzero long time signal in Figure 3, to a decreased δ absorption following hydrogen bond dissociation and the decay of this decreased absorption to the reformation of the transiently broken hydrogen bonds.

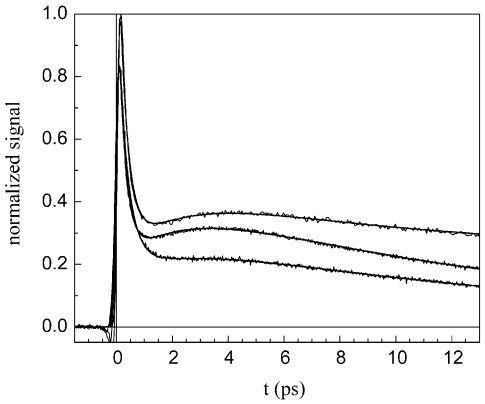

Figure 2. Short time pump−probe data for 2.5 (bottom curve), 5 (middle curve), and 26 (top curve) mol % samples of methanol-*d* in CCl_4. The solid lines show the fits to the kinetic model.

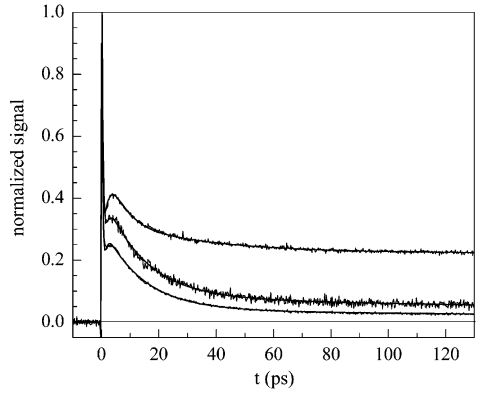

Figure 3. Long time pump−probe data for 2.5 (bottom curve), 5 (middle curve), and 26 (top curve) mol % samples of methanol-*d* in CCl_4. The solid lines show the fits to the kinetic model.

Consider a subensemble of vibrationally excited δ methanol molecules, that is, molecules that both accept and donate hydrogen bonds. If vibrational relaxation leads to hydrogen bond breaking in some fraction of this subensemble, the dissociation of hydrogen bonds will lead to a decreased number of methanol molecules participating in two hydrogen bonds. Spectroscopically, this will result in a decreased absorption at ∼2500 cm^{-1} and an increased pump−probe signal. The manner in which hydrogen bond breaking leads to a decreased δ population can be pictured as follows. For a trimer, the shortest oligomer with at least one δ absorber, dissociation of a hydrogen bond results in the elimination of the δ methanol and the formation of a methanol monomer (α methanol). The remaining dimer has a β and a γ methanol. For longer oligomers, a similar process can occur whereby dissociation of the hydrogen bond to the methanol at either end of the oligomer leads to the formation of a monomer and the elimination of a δ methanol. Alternatively, dissociation of an internal hydrogen bond in an oligomer will result in the formation of two shorter oligomers. This results in the transformation of two internally bound molecules into two terminal molecules and the elimination of two δ absorbers. In all cases, hydrogen bond dissociation leads to a reduced population of absorbers at ∼2500 cm^{-1}.

A kinetic model has been constructed to describe this complex sequence of population dynamics. The initial relaxation of the vibrational excited state follows a simple exponential decay

$$\frac{dN_e(t)}{dt} = -k_r N_e(t) \qquad (1)$$

where k_r is the rate for vibrational relaxation and $N_e(t)$ is the vibrationally excited state concentration. Equation 1 has the solution

$$N_e(t) = N_e(0)e^{-k_r t} \tag{2}$$

These vibrationally excited molecules can be separated into five fractional populations whose sum equals unity: (i) those that return to the ground vibrational state without breaking hydrogen bonds, F_g; (ii) those that return to the ground state and both break and reform hydrogen bonds fast, F_{ff}; (iii) those that return to the ground state and both break and reform hydrogen bonds slowly, F_{ss}; (iv) those that return to the ground state and break hydrogen bonds fast that reform slowly, F_{fs}; and (v) those that return to the ground state and break hydrogen bonds slowly that reform fast, F_{sf}. The actual populations correspond to the product of the fractional populations and the excited state concentration, FN_e. In contrast to the predissociative models for vibrational relaxation and hydrogen bond dissociation,[16,23,24] we do not assume that hydrogen bond dissociation and vibrational relaxation are simultaneous, a distinction that will be addressed in greater detail shortly.

Vibrational relaxation of the N_e population leads to hydroxyl stretch ground state molecules that go on to dissociate hydrogen bonds. These populations temporarily reside in a configuration, labeled with a superscript *, that cannot be distinguished experimentally from those vibrationally relaxed molecules that do not lead to hydrogen bond breaking, $N_g = N_e F_g$. Four such intermediate populations exist as follows: N^*_{gff} for molecules that both break and reform hydrogen bonds fast, N^*_{gfs} for molecules that break fast and slowly reform hydrogen bonds, N^*_{gsf} for molecules that slowly break hydrogen bonds that reform fast, and N^*_{gss} for those that break and reform hydrogen bonds slowly. N^*_{gff} and N^*_{gfs} decay with the fast hydrogen bond breaking rate, k_{bf}, while N^*_{gsf} and N^*_{gss} decay with the slow hydrogen bond breaking rate, k_{bs}. Those molecules that dissociate hydrogen bonds can be observed experimentally and will be represented by N_{gff}, N_{gfs}, N_{gsf}, and N_{gss} where the subscript definitions described above apply. The populations N_{gff} and N_{gsf} ultimately decay to the ground state N_g with the hydrogen bond reformation rate, k_f, while the populations N_{gfs} and N_{gss} will decay to N_g with the hydrogen bond reformation rate, k_s. The detailed population dynamics for N^*_{gff} can be represented by the following differential equations

$$\frac{dN^*_{gff}(t)}{dt} = F_{ff}k_r N_e(t) - k_{bf}N^*_{gff}(t) \tag{3}$$

$$\frac{dN_{gff}(t)}{dt} = k_{bf}N^*_{gff}(t) - k_f N_{gff}(t) \tag{4}$$

Kinetic equations of the same form apply to the other populations N_{gfs}, N_{gsf}, and N_{gss}.

The observed signal is given by

$$S(t) = 2N_e(t) + N_{gff}(t) + N_{gfs}(t) + N_{gsf}(t) + N_{gss}(t) \tag{5}$$

The factor of 2 in front of the first term on the right-hand side reflects the equal contributions to the pump−probe signal that arise from vibrationally excited molecules due to reduced ground state absorption (bleaching) and stimulated emission. The second through fifth terms describe hydroxyl stretch ground state populations that have broken a hydrogen bond. They do not have a factor of 2 because stimulated emission only occurs from molecules in the excited state. The solution to these differential equations results in the following expression for the pump−probe signal

$$\begin{aligned} S(t) = {} & 2Q(N_e(0)e^{-k_r t}) + \\ & Q\left(\frac{F_{ff}N_e(0)k_r k_{bf}}{(k_{bf}-k_f)(k_f-k_r)(k_{bf}-k_r)}\right)\{(k_{bf}-k_f)e^{-k_r t} + \\ & (k_f-k_r)e^{-k_{bf}t} - (k_{bf}-k_r)e^{-k_f t}\} + \\ & Q\left(\frac{F_{fs}N_e(0)k_r k_{bf}}{(k_{bf}-k_s)(k_s-k_r)(k_{bf}-k_r)}\right)\{(k_{bf}-k_s)e^{-k_r t} + \\ & (k_s-k_r)e^{-k_{bf}t} - (k_{bf}-k_r)e^{-k_s t}\} + \\ & Q\left(\frac{F_{sf}N_e(0)k_r k_{bs}}{(k_{bs}-k_f)(k_f-k_r)(k_{bs}-k_r)}\right)\{(k_{bs}-k_f)e^{-k_r t} + \\ & (k_f-k_r)e^{-k_{bs}t} - (k_{bs}-k_r)e^{-k_f t}\} + \\ & Q\left(\frac{F_{ss}N_e(0)k_r k_{bs}}{(k_{bs}-k_s)(k_s-k_r)(k_{bs}-k_r)}\right)\{(k_{bs}-k_s)e^{-k_r t} + \\ & (k_s-k_r)e^{-k_{bs}t} - (k_{bs}-k_r)e^{-k_s t}\} \end{aligned} \tag{6}$$

where Q is a normalization parameter.

The fits of eq 6 to the data acquired for the several concentrations of methanol-*d* dissolved in CCl_4 appear in Figures 2 and 3, and the parameters extracted from the fits are given in Table 1. While the fits involve a large number of parameters, the errors in the reported values demonstrate the relative independence of the rate parameters. The reformation rates, k_s and k_f, occur on time scales distinct from all other dynamic events and can therefore be determined accurately. The two breaking rate constants, k_{bf} and k_{bs}, differ by an order of magnitude and are essentially independent. The similar rates for k_{bf} and k_r make these values interdependent, as reflected in the elevated errors for these parameters.

The dynamics observed for all three concentrations of methanol-*d* strongly resemble one another, with one important exception. The fraction of excited molecules that proceeds to break and then reform hydrogen bonds slowly, $F_{fs} + F_{ss}$, increases with increasing concentration due to a concentration-dependent change in the sample temperature, as will be discussed shortly.

A particularly important aspect of the fits is the necessity for two hydrogen bond breaking rates. The slow hydrogen bond breaking process is indirect; it is a relatively slow process that need not break the hydrogen bond of the initially excited molecule. This fact was demonstrated by experiments in which β methanols (nonhydrogen bond donors) were excited and hydrogen bonds broke with almost the identical rate as observed here for excitation of δ methanol.[26] The fast hydrogen bond dissociation observed for δ methanol did not appear in experiments on β methanol. While the fast bond breaking proceeds with a rate constant larger than the rate constant for vibrational relaxation, the bond breaking still occurs after vibrational relaxation. As discussed further below, this is in contrast to a mechanism in which vibrational relaxation and hydrogen bond breaking are a single process.[16,23,24] The necessity of including the fast process in the model can be seen by viewing Figure 4. The best fit to the signal with a single dissociation rate underestimates the signal at the first minimum and overestimates the rate with which the second signal maximum occurs. This is a clear systematic error. No adjustment of the parameters with

TABLE 1: Parameters Extracted from Fit to Eq 6

	k_r^{-1} (fs)	k_{bf}^{-1} (fs)	k_{bs}^{-1} (ps)	k_f^{-1} (ps)	k_s^{-1} (ns)	F_{gff}	F_{gfs}	F_{gsf}	F_{gss}
2.5 mol % methanol-*d*	390 ± 50	250 ± 50	2.6 ± 0.6	14 ± 2	≫10	0.05	0.01	0.08	0.01
5.0 mol % methanol-*d*	340 ± 50	300 ± 100	2.3 ± 0.4	14 ± 3	≫10	0.10	0.02	0.10	0.02
26 mol % methanol-*d*	360 ± 60	200 ± 50	1.6 ± 0.4	12 ± 3	≫10	0.11	0.06	0.14	0.16

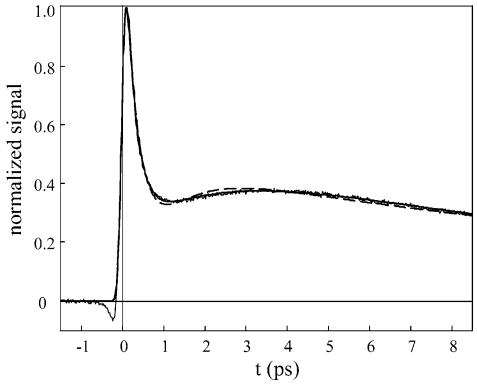

Figure 4. Fit of the 5 mol % methanol-*d* data to a kinetic model with one (- -) and two (—) hydrogen bond dissociation times. The fit with only one hydrogen bond dissociation time underestimates the signal at the first minimum, has a second maximum that peaks too early in time, and results in a 50% increase in the χ^2 for the fit.

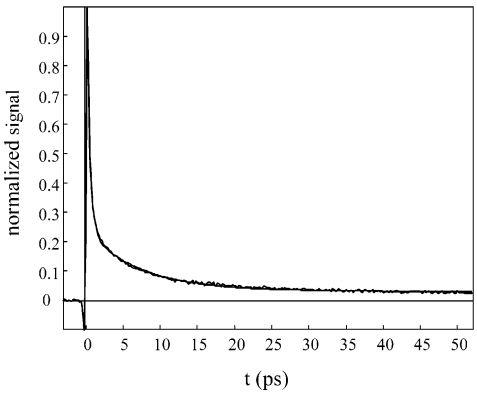

Figure 5. Data for the isotopically mixed sample, 0.8 mol % methanol-*d*/23 mol % methanol-*h* in CCl_4, and a fit to the kinetic model. The absence of the second maximum in the pump−probe signal clearly distinguishes the dynamics that can be observed in the isotopically mixed sample from those of the isotopically pure methanol-*d*/CCl_4 solutions.

a single breaking time can correct the mismatch between the data and the calculations. Using a single breaking rate results in a 50% increase in χ^2.

The fit of eq 6 to the 0.8 mol % methanol-*d*/23 mol % methanol-*h* in CCl_4 data appears in Figure 5. The absence of the second maximum in the pump−probe signal clearly distinguishes the isotopically mixed dynamics from those of the isotopically pure methanol-*d*. The initial relaxation proceeds with a time constant of $k_r^{-1} = 430 \pm 70$ fs. Following vibrational relaxation, hydrogen bond dissociation occurs with a time constant of $k_{bf}^{-1} = 220 \pm 40$ fs. These rates strongly resemble those observed for the pure methanol-*d* in CCl_4. The hydrogen bond reformation time constants have also been measured, with $k_f^{-1} = 7.4 \pm 0.6$ ps and $k_s^{-1} \gg 10$ ns. For a successful fit of the data to eq 6, the combined magnitude of the populations that slowly break hydrogen bonds following vibrational relaxation, $F_{sf} + F_{ss}$, must be roughly an order of magnitude smaller than those observed for the isotopically pure samples. A potential explanation for this difference and the faster rate of hydrogen bond reformation for the isotopically mixed methanol sample will be addressed in the following section.

B. Discussion. By fitting the experimental data to the above kinetic model, the time scales for a wide range of events in strongly hydrogen-bonded methanol have been identified. Here, we discuss the physical origin of these rates and construct a mechanism for hydrogen bond dissociation and reformation consistent with these experimental findings, as well as those of complementary experimental and theoretical studies.

The frequency-dependent hydroxyl stretch excited state lifetimes that we measured resembled those measured previously by Laenen et al. for methanol-*h* in CCl_4[21] and those measured by Woutersen et al. for ethanol-*h* in CCl_4.[23] In contrast, the lifetime of a deuterated hydroxyl stretch that accepts but does not donate a hydrogen bond (β-methanol) exceeds that of a deuterated hydroxyl stretch participating in two hydrogen bonds by a factor of ~4.5.[25,26] Clearly, donation of a hydrogen bond greatly increases the rate of vibrational decay. While this has been observed previously,[30] no thorough explanation for this effect has been achieved. Previous theoretical and experimental studies attributed the fast rate of decay to direct relaxation into the hydrogen bond coordinate.[16,23,24] In addition to explaining the fast relaxation, this mechanism also accounts for the fast dissociation of hydrogen bonds observed experimentally following vibrational excitation of hydroxyl stretches.[9,16−23] Subsequent theoretical and experimental studies have failed to support the direct relaxation of the hydroxyl stretch into the hydrogen bond coordinate.[12,31,32]

In a molecular dynamics simulation, Staib found that limiting the hydroxyl stretch decay to rotations, translations, and intermolecular modes such as the hydrogen bond vibration resulted in an excited state lifetime many orders of magnitude longer than the experimentally measured lifetimes.[12] Staib concluded from this work that relaxation to intramolecular vibrations determined the rate of hydroxyl stretch excited state decay. The experimental work of Iwaki and Dlott further supports this conclusion.[32] They observed the subsequent excitation of all intramolecular modes of methanol on the picosecond time scale following OH stretch excitation in liquid methanol. For water, excitation transfer to the bend overtone appears to determine the rate of hydroxyl stretch relaxation.[31,33] If a similar mechanism applies for methanol, hydrogen bond formation would still significantly influence the relaxation rate by changing the energy of the vibration and providing a strongly coupled energy sink for a fraction of the excitation energy. All of the vibrational energy need not go into the hydrogen bond coordinate for the initial relaxation to result in the direct dissociation of a hydrogen bond. Obviously, the excitation of OD bends, torsions, and librations as well as CO stretches would strongly influence the hydrogen bond length and angle as well.

Following vibrational relaxation, we observe hydrogen bonds dissociating on two time scales for the pure methanol-*d* in CCl_4 and one time scale for the 0.8 mol % methanol-*d*/23 mol % methanol-*h* in CCl_4. Both types of solutions undergo hydrogen bond breaking with a 220 fs time constant. The rate of this

breaking strongly suggests that the dissociation mechanism is direct, that is, the modes to which the excited hydroxyl stretch decays directly results in hydrogen bond dissociation. However, direct should not be confused with instantaneous, as the data and analysis demonstrate that all routes to hydrogen bond dissociation occur sequentially. The direct nature of the hydrogen bond breaking agrees with the predictions of the predissociative mechanism for vibrational decay and bond breaking.[16,23,24] Even for the predissociative mechanism, the rate of hydrogen bond dissociation should not be instantaneous. Unlike previous experimental studies, our data have yielded the time scale for this direct hydrogen bond dissociation, whereas previous studies have assumed the dissociation to be instantaneous.

Given the significantly higher vibrational frequency of the OD stretch, $\sim$2500 cm^{-1}, as compared to the hydrogen bond stretch, $\sim$200 cm^{-1}, an adiabatic separation can be made between the high frequency hydroxyl stretch and the lower frequency hydrogen bond vibration. This adiabatic separation results in the vertical decay of the hydroxyl stretch in the hydrogen bond coordinate; the length of the hydrogen bond does not change the instant the excited hydroxyl stretch decays. The predissociative mechanism predicts that solvation dynamics in the excited state will shorten the hydrogen bond.[24,34] Vibrational relaxation from the solvated excited state thus results in a vertical transition to a hydrogen bond length shorter than that of the ground state equilibrium configuration. The initial nonequilibrium configuration will result in wave packet evolution on the ground state potential energy surface, with the time scale for wave packet evolution determining the time scale for hydrogen bond breaking. As a rough estimate, the time for wave packet evolution and hydrogen bond dissociation should be related to one-half the period of oscillation in the hydrogen bond potential. Given a hydrogen bond frequency of $\sim$200 cm^{-1},[24] the half period should be roughly 100 fs, providing the correct order of magnitude for the fast hydrogen bond dissociation. The deviation between the time constant for dissociation and the half period of hydrogen bond vibration may reflect the fact that motion on the hydrogen bond potential will be highly anharmonic and damped.

While the above discussion focuses on the hydrogen bond length, a similar mechanism may exist in which solvation in the excited state modifies the hydrogen bond angle with direct dissociation following OD stretch relaxation to excited OD bends, torsions, or methanol librations. Vibrational studies of water trimers in the gas phase show the lifetime of the hydrogen bond to be 1$-$6 ps following the excitation of a libration, a lifetime roughly 3 orders of magnitude shorter than that measured following the excitation of either a translational or a torsional vibration.[35,36]

In the isotopically mixed 0.8 mol %/methanol-*d* 23 mol % methanol-*h* solution, the initial relaxation results in a decreased absorption like that observed for the isotopically pure solution, but unlike the isotopically pure sample, no second maximum occurs (compare Figures 3 and 5). Fitting of the data to the kinetic model utilized for the isotopically pure methanol-*d* in CCl_4 data demonstrates that the fast dissociation observed in pure methanol-*d* also appears in the isotopically mixed sample with close to the same magnitude and rate constant. The slow dissociation, however, occurs with an order of magnitude smaller amplitude than that observed in the isotopically pure solutions.

We propose that the slower hydrogen bond breaking observed in isotopically pure methanol-*d* following the vibrational relaxation of δ methanol occurs via an indirect energy relaxation as has been observed for experiments on β methanol.[25,26] The absence of this rate of hydrogen bond breaking in the isotopically mixed methanol solution supports this conclusion. In the isotopically pure solution, dissociation of any hydrogen bond will influence the signal, while in the isotopically mixed sample only the dissociation of hydrogen bonds involving a deuterated hydroxyl stretch will contribute to the signal. In the isotopically mixed sample, only one out of thirty methanol molecules can absorb at $\sim$2500 cm^{-1}. Consequently, virtually no oligomers in the isotopically mixed sample have more than one absorber. This effectively makes all but the excited molecule within the oligomer invisible to the laser radiation. The absence of the slower dissociation rate for the isotopically mixed sample suggests that the slower dissociation occurs after the initial excitation energy has spread over a number of methanol molecules within the oligomer. While this represents an unexpectedly fast rate of intermolecular energy redistribution, the presence of strong intermolecular hydrogen bonds makes a greatly enhanced rate of intermolecular energy transfer plausible.

The reformation of dissociated hydrogen bonds represents the final stage of energy relaxation observed in the pump$-$probe signal. This reformation results in a long time offset that decays on a time scale longer than 100 ps. We attribute this offset to a finite temperature change within the excited volume of the sample, consistent with our interpretation of the long time offset observed for excitation of β methanol-*d*.[26] The local vibrational energy content of the hydrogen-bonded network increases following vibrational relaxation. The initial dissociation of hydrogen bonds results in decreased absorption at $\sim$2500 cm^{-1}, as discussed above. Recombination of hydrogen bonds causes this signal to decay. Energy transfer through the hydrogen-bonded methanol oligomer does not result in the full equilibration of the sample. The initially excited oligomers have a greater probability of finding a hydrogen bond broken than under the thermal equilibrium conditions of the sample at the initial temperature. While not yet equilibrated, the excited oligomers can be qualitatively thought of as being "hot" due to elevated levels of internal energy. These hot oligomers relax further. This relaxation occurs on roughly two time scales, $k_f^{-1} \approx 13$ ps and $k_s^{-1} \gg 10$ ns. Previous studies of this relaxation in methanol-*d*, ethanol-*d*, and 1-propanol-*d* demonstrated that these rates of relaxation do not vary with molecular species.[26] The lack of variation in fast recombination rates for the different alcohols studied suggests that the time scale observed does not represent the time for oligomer reorganization, since mechanical[37,38] and dielectric[39] reorganization dynamics of methanol, ethanol, and 1-propanol differ significantly. Alternatively, these dynamics could involve the time for CCl_4 reorganization or the time for energy transfer from the hydrogen-bonded oligomers to the CCl_4 solvent. The fast hydrogen bond reformation rates resemble the rate of energy transfer from methanol to CCl_4 observed by Iwaki and Dlott.[32] In the experiments of Iwaki and Dlott on a 25 mol % CCl_4 in 75 mol % methanol, the increase in the anti-Stokes Raman signal from CCl_4 following the vibrational excitation of the OH stretch of methanol was complete within 50 ps, which provides a measure of the local thermal equilibration time. It is reasonable to assume that the fast recovery of hydrogen bonds involves equilibration of the nonequilibrium distribution of vibrations and the flow of vibrational energy out of the initially excited oligomer into the CCl_4 solvent. Approximately 1 in 100 δ methanol-*d* molecules are initially excited. As energy leaves the initially excited oligomers and spreads through the solvent, the "local temperature" decreases, leading to the reformation of hydrogen bonds. Approximate calculations based on the rate

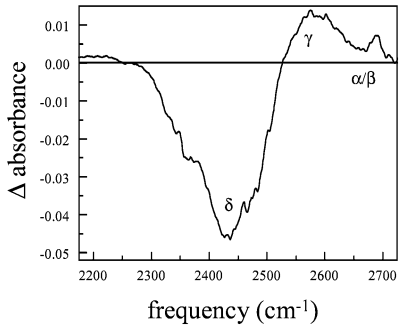

Figure 6. Temperature-dependent difference spectrum for 26 mol % methanol-*d* in CCl_4. The plot shows the change in absorbance for a 294 K spectrum subtracted from a 301 K spectrum. Negative changes in absorbance will result in a positive pump−probe signal. The α, *β*, and *γ* increased absorbance and the *δ* decreased absorbance result from a reduced equilibrium number of hydrogen bonds.

of thermal diffusion in CCl_4 show that the time scale for macroscopic thermal equilibration within the laser spot occurs on the order of 100 ps, consistent with the time for the completion of the observed fast decay from the second maximum.

Within this picture, the slowly recovering offset results from the finite temperature change within the volume of vibrational excitation by the laser. The equilibrium properties of the hydrogen-bonded oligomers in CCl_4 have significant temperature dependence. Figure 6 shows the steady state temperature-dependent difference spectrum for the 26 mol % methanol-*d* solution that results from a 7 K temperature increase from 294 to 301 K. The increase in temperature results in a decrease in the *δ* methanol absorption and an increase in the *γ* and α/*β* methanol absorptions. Calculations for a 26 mol % methanol-*d* sample indicate that the temperature rise associated with the absorption of IR photons once equilibration has occurred in the laser irradiated spot is ∼0.1 K. This temperature rise will leave the system with more broken hydrogen bonds and, therefore, less absorption at the *δ* peak frequency than before laser irradiation. The temperature rise will decay by thermal diffusion out of the laser-irradiated spot, which is very long as compared to the maximum delay in the experiments, 300 ps. Therefore, the slow component does not appear to decay at all. The concentration dependence of the long time signal offset further supports the assignment of this feature to an increased temperature within the laser spot. As shown in Figure 3, the magnitude of the offset increases with increasing concentration. As the concentration increases, the energy deposited per unit volume will increase. This will produce an increased temperature rise and a signal offset that increased roughly linearly with increasing concentration, as seen experimentally.

Attributing the long time positive offset to a temperature change provides further support for assigning the faster recombination rate, k_f, to the local equilibration rate, as it provides the rate with which the sample approaches local thermal equilibrium. The influence of a finite temperature change following vibrational excitation in hydrogen-bonded liquids has been observed by Laenen et al.,[20] as well as Lock et al.[40] In both cases, the average number of hydrogen bonds in the solution decreases with increasing temperature, resulting in an increased population of alcohol molecules that do not participate in two hydrogen bonds, namely, α, *β*, and *γ* species.

A question arises regarding the rate of hydrogen bond reformation; if thermal equilibration within the laser excitation volume yields alcohol-independent hydrogen bond reformation rates, why does the reformation of hydrogen bonds following excitation of *δ* methanol-*d* occur almost two times faster than following the excitation of *β* methanol-*d*?[25,26] Further inspection of the relaxation to the long time offset in the pump−probe signal for excitation of *δ* absorbers clearly demonstrates that this final relaxation does not have the functional form of a single-exponential decay, which was used in the model that led to eq 6 for simplicity. The $k_f^{-1} \approx 13$ ps time constant represents an average decay time for a biexponential relaxation. To account for the discrepancy between the data and the kinetic model, we constructed a slightly modified version of the model in which those hydrogen bonds that broke with the k_{bf} rate constant had a different rate constant for the fast recovery than those hydrogen bonds that broke with the k_{bs} rate constant. Fitting the 2.5 mol % methanol-*d* solution signal to the modified model gave the following results: hydrogen bonds that broke with the k_{bf} rate constant recovered with a time constant of $k_{ff}^{-1} = 7 \pm 3$ ps and hydrogen bonds that broke with the k_{bs} rate constant recovered with a time constant of $k_{sf}^{-1} = 20 \pm 3$ ps. The higher concentration methanol-*d* solutions show similar results. These results indicate that hydrogen bonds that broke via the slower, indirect mechanism recover with the rate of thermal equilibration within the laser excitation volume, a process that does not depend on either the alcohol or the species of hydroxyl stretch excited.

While appearing to complicate the situation, this provides a potential explanation for the rate of hydrogen bond reformation in the isotopically mixed solution. For excitation of *δ* absorbers in the isotopically mixed methanol sample, direct hydrogen bond dissociation, without a substantial amount of indirect OD bond breaking, leads to hydrogen bond reformation with a single-exponential time constant of $k_f^{-1} = 7.4 \pm 0.6$ ps. For excitation of *β* absorbers in methanol-*d*, hydrogen bond dissociation, without direct bond breaking, leads to hydrogen bond reformation with a single-exponential time constant of $k_f^{-1} = 23 \pm 8$ ps.[26] For excitation of *δ* absorbers in methanol-*d*, both direct and indirect hydrogen bond breaking contributes to the signal and the recovery of hydrogen bonds that occur with two exponential time constants of ∼7 and ∼20 ps with the constraint that directly dissociated bonds recover with the ∼7 ps time constant and indirectly dissociated bonds recover with the ∼20 ps time constant. This indicates that the different mechanisms for hydrogen bond breaking have different mechanisms for hydrogen bond reformation. Within this context, hydrogen bonds broken by the indirect route recover with the rate of thermal equilibration within the excited sample volume, while structural reorganization of the oligomer appears to determine the rate of hydrogen bond recovery for bonds broken by the direct route.

Studies of vibrational relaxation in 5 mol % ethanol-*d* dissolved in CCl_4 have also been conducted. All stages of the relaxation occur with very similar rates to those observed for methanol-*d*. The signal and the fit of the signal to eq 6 appear in Figure 7. The following time constants have been extracted from the fit to the data: $k_r^{-1} = 340 \pm 50$ fs, $k_{bf}^{-1} = 170 \pm 50$ fs, $k_{bs}^{-1} = 2.8 \pm 0.6$ ps, $k_f^{-1} = 15 \pm 3$ ps , and $k_s^{-1} \geq 10$ ns. As seen for the isotopically pure methanol-*d* solutions, the ∼15 ps time constant for hydrogen bond recovery corresponds to an average rate of recovery for a nonexponential relaxation. The faster component of the recovery can be more accurately fit with two hydrogen bond reformation rates with time constants of ∼7 and ∼20 ps, with the slow component ≫10 ns. These data for ethanol-*d* further demonstrate that a characteristic sequence of hydrogen bond breaking and reformation events following vibrational relaxation occurs for small molecule

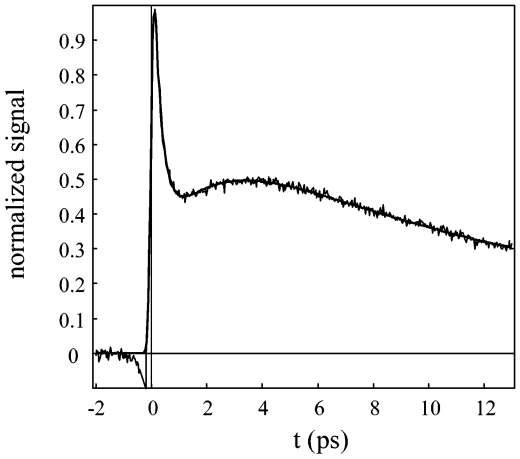

Figure 7. Short time pump−probe data for a 5 mol % solution of ethanol-*d* in CCl_4. The smooth curve is the fit to the kinetic model. The parameters obtained from the fit are very similar to those obtained for methanol-*d*.

alcohol solutions with rates that generally depend little upon the molecular species or the concentration.

IV. Orientational Relaxation and Spectral Diffusion

In the data analysis presented above, orientational relaxation, vibrational excitation transfer, and spectral diffusion were not included in the discussions of the dynamics. These are interesting effects that provide additional information on the dynamics that occur in hydrogen-bonding systems. However, as will be shown below, they do not change the analysis or the interpretation presented above. The influences of these effects on the data basically fall within the error bars of the measurements.

A. Orientational Relaxation and Vibrational Excitation Transfer. The decay of polarization anisotropy in liquids can be determined by measuring the probe polarization dependence of the pump−probe signal. By measuring the pump−probe anisotropy decay for both isotopically pure and isotopically dilute solutions of methanol, the rates of vibrational excitation transfer and molecular reorientation can be investigated. The experiments were performed on both a 26 mol % methanol-*d* solution and a 0.8 mol % methanol-*d*/23 mol % methanol-*h* in CCl_4 solution. In the sample with low methanol-*d* concentration, vibrational excitation transfer does not occur because of the very large separation between methanol-*d* molecules (see below). Therefore, any anisotropy decay results from orientational relaxation. The difference between the dilute and the concentrated deuterium samples can be attributed to vibrational excitation transfer.

Frequently, the anisotropy decay is determined by measuring the time-dependent signals with the probe pulse parallel to and perpendicular to the pump polarization. Alternatively, the anisotropy decay can be determined by measuring the time-dependent probe intensity with the probe parallel to and rotated 54.7° (the magic angle) from the pump polarization.[41] We have employed the latter approach to measure the anisotropy in these systems.

Excitation of the sample by the linearly polarized pump pulse results in a $\cos^2\theta$ distribution of vibrationally excited molecules, where θ represents the angle between the transition dipole moment and the pump polarization vector. For excitation of a hydroxyl stretch, the transition dipole moment will be directed along the OD bond. When the probe pulse has the same linear polarization as the pump pulse, reorientation of the hydroxyl group of methanol-*d* or excitation hopping,[41−45] which transfers

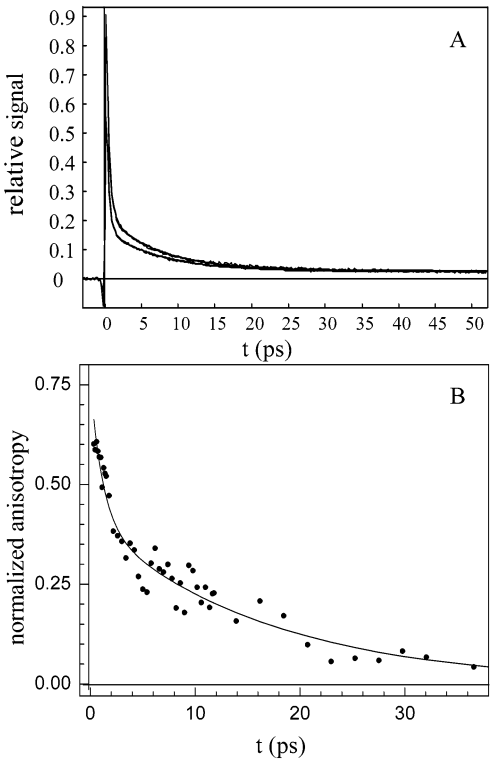

Figure 8. (A) Pump−probe signal collected with the probe parallel and at the magic angle with respect to the pump polarization. (B) The normalized anisotropy decay for 0.8 mol % methanol-*d*/23 mol % methanol-*h* dissolved in CCl_4. The anisotropy decays as a biexponential with time constants of 1.7 ± 0.7 and 17 ± 3 ps.

the excitation to another hydroxyl having its transition dipole pointing in a different direction, will result in a diminished signal. For a probe polarization rotated 54.7° from the polarization of the pump, polarization anisotropy relaxation is eliminated from the signal.[41] The parallel, $S_{\|}(t)$, and magic angle, $S_{ma}(t)$, signals can be utilized to determine the time-dependent anisotropy[41]

$$R(t) = \frac{S_{\|}(t) - S_{ma}(t)}{2S_{ma}(t)} \tag{7}$$

which has a theoretical maximum value of 0.4 that decays to zero.

The parallel and magic angle pump−probe, as well as the anisotropy signals, appear in Figure 8 for the 0.8 mol % methanol-*d*/23 mol % methanol-*h* in CCl_4. Similar data appear in Figure 9 for the 26 mol % methanol-*d* in CCl_4. The isotopically mixed solution displays a biphasic decay, with time constants of 1.7 ± 0.7 and 17 ± 3 ps. The anisotropy decay for the 26 mol % methanol-*d* can be fit with a single time constant of 860 ± 80 fs. Two primary distinctions exist between the anisotropy data collected for the two samples: the anisotropy relaxation for the 26 mol % methanol-*d* sample can be fit to a single-exponential decay, rather than a biexponential decay, and the anisotropy decays twice as fast as the fast component of the orientational relaxation in the isotopically mixed sample.

First, consider the isotopically mixed sample (Figure 8). For a transition dipole−transition dipole interaction (Förster mechanism), the rate of excitation transfer falls off as $1/r$,[6] where r is the intermolecular separation.[46] For other mechanisms such as exchange coupling, the rate of transfer has an even steeper dependence on distance. The low methanol-*d* concentration in the isotopically mixed sample creates a large average distance

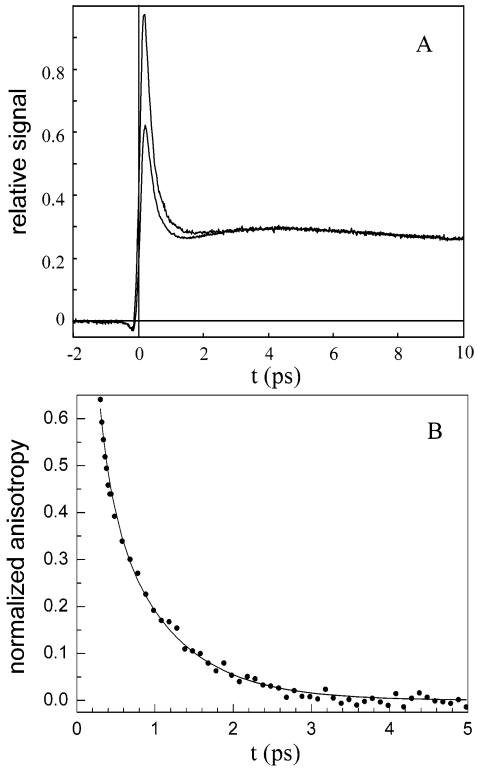

Figure 9. (A) Pump−probe signal collected with the probe parallel and at the magic angle with respect to the pump polarization. (B) The normalized anisotropy decay for 26 mol % methanol-*d* dissolved in CCl_4. The anisotropy decays exponentially with a time constant of 860 ± 80 fs.

between δ OD stretches, reducing the vibrational excitation transfer rate to a negligible level. As will be discussed in detail in another paper,[28] the two time scales of the orientational relaxation can be attributed to a fast, restricted relaxation (wobbling in a cone)[47,48] and full orientational diffusion leading to complete randomization on the longer time scale. The time constant for both components of the decay is in reasonable agreement with previous dielectric relaxation measurements.[49]

In the isotopically pure sample, the methanol-*d* molecules are in close proximity, and excitation transfer provides a possible route for anisotropy decay. The anisotropy decay observed in the isotopically pure sample (Figure 9) is a combination of the orientational relaxation observed in the isotopically mixed sample and the additional depolarization caused by excitation transfer.[45] The problem of excitation transfer among many identical molecules randomly distributed in solution is complex, but it has been solved in considerable detail.[44] In the situation that will occur in a hydrogen-bonded oligomer, it is not safe to assume that either the distribution of distances or the relative orientations of the chromophores is random. The excitation transfer in this system will be discussed in detail in a subsequent publication[28] where it will be shown that combining an approximate description of excitation transfer[42,43,50] with the measured orientational relaxation can reproduce the data. For our purposes here, it is sufficient to obtain the time scale of excitation transfer by assuming that the excitation transfer-induced depolarization can be modeled as an exponentially decaying process. An excitation transfer time constant of 1.2 ps best reduces the biexponential orientational relaxation found for the isotopically mixed solution to the single-exponential decay observed for the pure methanol-*d* in CCl_4 sample.

Excitation transfer in hydrogen-bonding systems has been discussed previously by Bakker and co-workers.[23,51] They

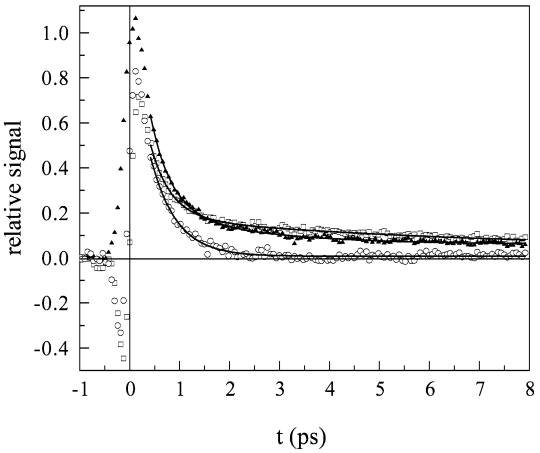

Figure 10. Frequency-resolved pump−probe signal collected at 2450 (□), 2510 (▲), and 2550 cm^{-1} (○) with the laser centered at 2515 cm^{-1} with an 85 cm^{-1} fwhm. The solid lines represent the fits of the data to the kinetic model.

observed instrument response-limited anisotropy decay for pure water and placed an upper bound on the relaxation time constant of <100 fs. They have attributed this fast anisotropy decay to vibrational excitation hopping. In the 26 mol % methanol-*d* in CCl_4 studied here, we observed significantly slower transfer. The overall rate of anisotropy decay from both excitation transfer and orientational relaxation in 26 mol % methanol-*d* in CCl_4 is slower than the initial decay of the pump−probe signal, which we assign to vibrational relaxation.

B. Spectral Diffusion. The evolution of the liquid structure surrounding a vibrational chromophore can result in spectral diffusion, that is, the time evolution of the vibrational transition frequency.[52] Transient hole burning provides an effective technique to investigate spectral diffusion.[18,34,53−56] When the absorption line width exceeds the laser bandwidth, fluctuations in the hydroxyl stretch environment and structural relaxation of the hydrogen-bonding network can result in spectral diffusion and a decay of the pump−probe signal. Thus, the time dependence of the frequency width and frequency maximum of the signal provide two spectroscopically measurable manifestations of the time-dependent evolution of the hydrogen-bonding structures in methanol-*d* dissolved in CCl_4. To determine the extent of spectral diffusion in the experiments reported here, we have frequency resolved the probe pulse to identify the wavelength dependence of the vibrational relaxation for 0.8 mol % methanol-*d*/23 mol % methanol-*h* dissolved in CCl_4. These studies allow us to investigate the dynamics of structural relaxation in the absence of excitation transfer.

Spectral diffusion can produce a pump−probe signal decay without population relaxation. Vibrational transient hole burning has been applied to the investigation of spectral diffusion dynamics in methanol dissolved in CCl_4 previously.[21] The frequency-resolved pump−probe experiments described in this article have been conducted to identify the extent to which the fast initial relaxation observed here results from spectral diffusion. Thus, we emphasize the frequency dependence of the initial relaxation. A more detailed presentation of our measurements of spectral diffusion will be presented subsequently.[29]

The time-dependent vibrational relaxation measured at 2450, 2510, and 2550 cm^{-1} for vibrational excitation at 2515 cm^{-1} appears in Figure 10. The total signal for short time delays has significant coherent contributions from phase and amplitude gratings,[57] which will be discussed in a future paper.[29] Because of the frequency-dependent magnitude of these different coherent contributions to the signal, we fit the relaxation dynamics

TABLE 2: Relaxation Time Constants for the Frequency-Resolved Pump−Probe Experiments

	2450 cm^{-1}	2470 cm^{-1}	2490 cm^{-1}	2510 cm^{-1}	2530 cm^{-1}	2550 cm^{-1}
k_r^{-1} (fs)	430 ± 90	460 ± 60	500 ± 100	450 ± 80	480 ± 80	510 ± 40
lifetime (fs) see text	420	430	460	530	700	900

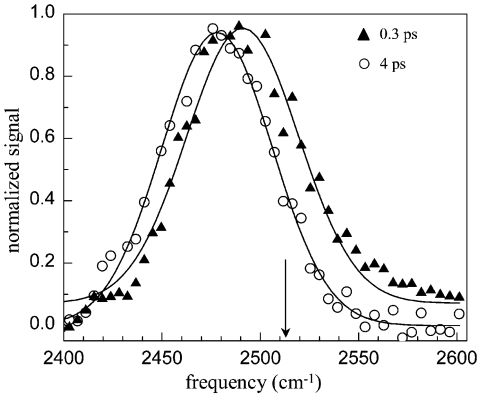

Figure 11. Frequency-resolved pump−probe spectra for 300 fs (▲) and 4 ps (○) time delays with the laser centered at 2515 cm^{-1} with an 85 cm^{-1} fwhm. The solid lines represent the fits of the data to single Gaussians.

only after a 400 fs time delay when the autocorrelation of the pump and probe pulses has decayed to roughly 1/20 of its maximum value and the coherent contributions to the signal have decayed to a negligible amplitude.

The first row of Table 2 presents the fast relaxation time constant measured at a variety of probe frequencies. As the probe frequency shifts from 2450 to 2550 cm^{-1}, the relaxation time lengthens. A similar frequency-dependent lifetime has been observed before for protonated methanol and ethanol dissolved in CCl_4.[21,23] A variation in the decay constant with wavelength has been discussed in terms of a wavelength-dependent population relaxation rate, where the population decay becomes faster as the wavelength is moved to the red.[21,23,24,32] However, we find that the lifetime does not shift monotonically. We observe a faster decay at 2510 cm^{-1} than at 2490 cm^{-1}. The faster decay at 2510 cm^{-1} than at 2490 cm^{-1} indicates that spectral diffusion occurs during the initial relaxation of the signal, resulting in a shift of the signal toward the red side of the absorption spectrum as shown in Figure 11. The frequency-dependent lifetime cannot explain this effect, as it would result in a blue shift of the transient absorption spectrum.

Despite the influence of spectral diffusion on the observed relaxation dynamics, the magnitude of the shift and broadening of the signal does not account for the majority of the fast initial decay (Figure 2). The extent of the influence of spectral diffusion on the initial fast relaxation was investigated using frequency-resolved pump−probe spectra taken at a variety of delay times. To obtain the spectrum of the hole and excited state, the frequency-resolved pump−probe signal must be divided by the attenuated probe laser spectrum to account for the variation of the probe intensity at each wavelength. The areas of the hole spectra were then normalized to unity, thereby eliminating the population decay. The normalized hole spectra display a time-dependent broadening and frequency shift. These time-dependent normalized spectra can be used to determine the contribution to the pump−probe decay at a given wavelength that arises solely from spectral diffusion.

A comparison of this calculated spectral diffusion only decay at 2510 cm^{-1} and the actual pump−probe signal decay at 2510 cm^{-1} is presented in Figure 12A. The calculated spectral diffusion only decay can be removed from the fast relaxation

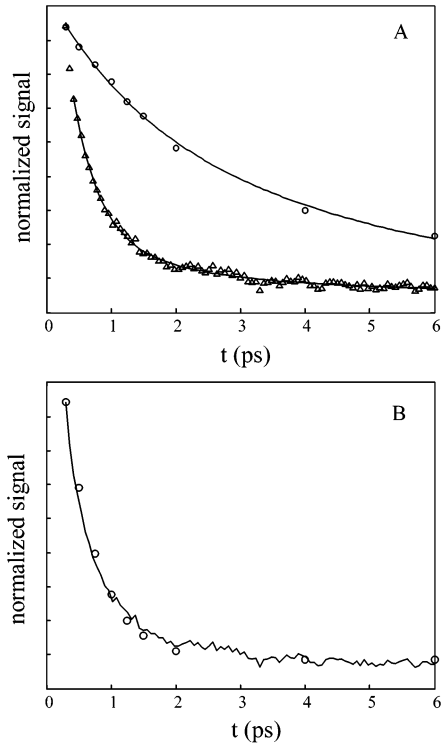

Figure 12. (A) Frequency-resolved data collected at 2510 cm^{-1} (△) as well as derived data at 2510 cm^{-1} that represent the signal decay due to spectral diffusion without vibrational relaxation (○). (B) Comparison of the frequency-resolved data at 2510 cm^{-1} (—) and the derived data in (A) multiplied by an exponential with a 530 fs lifetime (○). The exponential lifetime accounts for the effect of excited state decay. The vibrationally excited state decays with a time constant of ∼500 fs at 2510 cm^{-1}. Values of the excited state lifetimes at other frequencies appear in Table 2.

to determine the vibrational lifetime in the absence of spectral diffusion. To do this at each wavelength, the calculated spectral diffusion decay is multiplied by an exponentially decaying function. The decay constant is adjusted to fit the experimental data. This procedure is demonstrated in Figure 12B for 2510 cm^{-1}. The solid line is the measured decay, and the circles are the calculated decay using a decay time of 530 fs. We apply the same procedure to all of the spectra collected for time delays between 300 fs and 2 ps with the extracted vibrational lifetimes listed in the second row of Table 2. The results show a significant monotonic decrease in the lifetime for increasingly redder wavelengths.

The question arises, to what extent does spectral diffusion influence the initial relaxation observed for the frequency-integrated dynamics measured with the pump−probe experiment? The frequency-integrated lifetime, the equivalent of the pump−probe lifetime measured without spectral resolution, can be calculated by weighting the vibrational lifetimes listed in Table 2 with the relative amplitudes of the initially generated pump−probe signal at the different frequencies. The relative amplitudes of the pump−probe signal for a delay time of 300 fs give an estimated frequency-integrated lifetime of ∼500 fs, as do the relative amplitudes for a 500 fs delay time. This should be compared to the 430 ± 70 fs time constant for the initial

relaxation for the frequency-integrated signal. While removing the spectral diffusion contribution to the initial relaxation decay time makes the decay longer, the change is relatively small and does not exceed the error in the measurement. The rates of orientational and spectral diffusion, as well as excitation transfer in the 26 mol % methanol-*d* in CCl_4 sample, cumulatively proceed at a rate over a factor of 2 more slowly than the initial relaxation of the pump−probe signal, demonstrating that vibrational population decay dominates the initial relaxation. In the data analysis of the vibrational relaxation/hydrogen bond breaking dynamics, we did not attempt to remove or separate the various factors that contribute to the fast relaxation as they do not influence the overall model or change the nature of the results. While the various factors could have some influence on the actual numbers that emerge, they will only influence the analysis of the short time scale dynamics, which have significant error bars in any case.

V. Concluding Remarks

The hydroxyl stretch relaxation dynamics of methanol-*d* dissolved in CCl_4 have been measured with ultrafast infrared pump−probe spectroscopy. In the studies described in this paper, we excited a subensemble of methanol-*d* molecules that both accept and donate hydrogen bonds. Relaxation of the first vibrationally excited state of the hydroxyl stretch dominates the initial stage of signal decay. Experiments probing the rates of spectral diffusion, orientational relaxation, and excitation transport in both 26 mol % methanol-*d* dissolved in CCl_4 and 0.8 mol % methanol-*d*/23 mol % methanol-*h* dissolved in CCl_4 support the assignment of the initial fast signal decay as arising principally from vibrational relaxation with a lifetime of ∼500 fs.

The initial vibrational relaxation results in a decreased absorbance that rises to a second maximum. The decay from the second maximum occurs on two time scales. We attribute the rise to the second maximum to hydrogen bond dissociation following vibrational relaxation, which decreases the concentration of methanol-*d* molecules that both accept and donate hydrogen bonds and produces the observed increase in signal. The decay from the second maximum is caused by hydrogen bond reformation. Using a set of coupled kinetic equations, the time constants for hydrogen bond dissociation and reformation have been determined. Hydrogen bond breaking occurs with ∼200 fs and ∼2 ps time constants. We attribute the fast rate to a direct breaking mechanism where the hydroxyl stretch decays into modes that directly result in the dissociation of a hydrogen bond. We attribute the slower rate of breaking to an indirect breaking mechanism wherein the dissociation of hydrogen bonds follows vibrational energy flow from the excited molecule to an extended portion of the excited oligomer. The fact that the slower dissociation mechanism is not observed in the isotopically mixed solution supports this conclusion. For the vast majority of oligomers in the isotopically mixed solution, the vibrationally excited molecule will be the only deuterated molecule in the oligomer. In the isotopically mixed oligomers, redistribution of the energy over an extended portion of the oligomer will tend to result in an OH rather than an OD hydrogen bond breaking. Because the experimental observables are only sensitive to OD dynamics, breaking of OH hydrogen bonds will not contribute to the signal.

In the methanol-*d* in CCl_4 solutions, the reformation of hydrogen bonds occurs on three time scales. The bonds that break directly recover with ∼7 ps and ≫10 ns time constants, while the bonds that break indirectly recover with ∼20 ps and ≫10 ns time constants. The ∼20 ps reformation time scale has also been observed for excitation of alcohols that accept but do not donate hydrogen bonds where only indirect hydrogen bond breaking occurs.[25,26] In the isotopically mixed methanol in CCl_4 solution, in which only the direct hydrogen bond dissociation dynamics can be observed, hydrogen bond reformation is observed with a single-exponential time constant of $k_f^{-1} = 7.4 \pm 0.6$ ps. This indicates that the mechanism by which hydrogen bonds dissociate determines the rate with which the bonds reform.

The population of indirectly dissociated hydrogen bonds reforms to an extent determined by the new local equilibrium temperature. The faster recovery of the population of directly dissociated hydrogen bonds rules out the assignment of this rate to temperature equilibration within the excited sample volume. As will be discussed in a future paper,[29] structural evolution within the oligomer determines the rate of this recovery. The slowly recovering component (≫10 ns) observed for both breaking mechanisms reflects the slow diffusion of thermal energy out of the laser excitation volume.

Experiments examining orientational relaxation, vibrational excitation transfer, and spectral diffusion provide insights into the dynamics of other processes associated with hydrogen-bonded methanol oligomers, which will be addressed in detail in later papers. For the purposes of the present paper, these contributions to signal decay have been discussed to demonstrate that vibrational excited state decay dominates the initial relaxation. For the case of an isotopically mixed solution of 0.8% methanol-*d*/23% methanol-*h* in CCl_4, where no excitation transfer occurs, roughly 90% of the initial signal relaxation reflects excited state decay. For the isotopically pure solutions of methanol-*d* in CCl_4 where excitation transfer does occur, >75% of the initial relaxation results from excited state decay. The conclusion that hydroxyl stretch excitation leads to hydrogen bond dissociation predates these experimental studies by many decades.[58] Despite numerous investigations,[9,16−23] the mechanism by which vibrational relaxation and hydrogen bond breaking occur has remained elusive. In the studies presented here, we have been able to identify that both direct and indirect mechanisms for hydrogen bond dissociation provide significant routes for hydrogen bond breaking and that both mechanisms occur after vibrational relaxation of the initially excited hydroxyl stretch. These results have clarified the variety of hydrogen bond breaking and reformation processes and their time scales. They provide a basis for a significantly enhanced understanding of the nature of molecular motions and couplings that lead to hydrogen bond dissociation and reformation.

Acknowledgment. This work was supported by the Department of Energy (Grant DE-FG03-84ER13251), the National Science Foundation (DMR-0088942), and the National Institutes of Health (1RO1-GM61137). N.E.L. gratefully acknowledges support for a sabbatical leave from the NSF POWRE program (CHE-0074913).

References and Notes

(1) Chandler, D. *J. Chem. Phys.* **1978**, *68*, 2959.
(2) Grote, R. F.; Hynes, J. T. *J. Chem. Phys.* **1980**, *73*, 2715.
(3) Frauenfelder, H.; Wolynes, P. G. *Science* **1985**, *229*, 337.
(4) Bagchi, B.; Fleming, G. R. *J. Phys. Chem.* **1990**, *94*, 9.
(5) Voth, G. A.; Hochstrasser, R. M. *J. Phys. Chem.* **1996**, *100*, 13034.
(6) Karplus, M. *J. Phys. Chem. B* **2000**, *104*, 11.
(7) Schuster, P.; Zundel, G.; Sandorfy, C. *The Hydrogen Bond. Recent Developments in Theory and Experiments*; North-Holland: Amsterdam, 1976.
(8) Henri-Rousseau, O.; Blaise, P. *Adv. Chem. Phys.* **1998**, *103*, 1.

(9) Graener, H.; Ye, T. Q.; Laubereau, A. *J. Chem. Phys.* **1989**, *90*, 3413.
(10) Liddel, U.; Becker, E. D. *Spectrochim. Acta* **1957**, *10*, 70.
(11) Symons, M. C. R.; Thomas, V. K. *J. Chem. Soc., Faraday Trans. 1* **1981**, *77*, 1883.
(12) Staib, A. *J. Chem. Phys.* **1998**, *108*, 4554.
(13) Kristiansson, O. *J. Mol. Struct.* **1999**, *477*, 105.
(14) Veldhuizen, R.; de Leeuw, S. W. *J. Chem. Phys.* **1996**, *105*, 2828.
(15) van den Broek, M. A. F. H.; Nienhuys, H. K.; Bakker, H. J. *J. Chem. Phys.* **2001**, *114*, 3182.
(16) Graener, H.; Ye, T. Q.; Laubereau, A. *J. Chem. Phys.* **1989**, *91*, 1043.
(17) Laenen, R.; Rauscher, C. *J. Chem. Phys.* **1997**, *107*, 9759.
(18) Laenen, R.; Rauscher, C.; Laubereau, A. *J. Phys. Chem. A* **1997**, *101*, 3201.
(19) Laenen, R.; Rausch, C. *J. Chem. Phys.* **1997**, *106*, 8974.
(20) Laenen, R.; Rauscher, C.; Laubereau, A. *Chem. Phys. Lett.* **1998**, *283*, 7.
(21) Laenen, R.; Gale, G. M.; Lascoux, N. *J. Phys. Chem. A* **1999**, *103*, 10708.
(22) Laenen, R.; Rauscher, C.; Simeonidis, K. *J. Chem. Phys.* **1999**, *110*, 5814.
(23) Woutersen, S.; Emmerichs, U.; Bakker, H. J. *J. Chem. Phys.* **1997**, *107*, 1483.
(24) Staib, A.; Hynes, J. T. *Chem. Phys. Lett.* **1993**, *204*, 197.
(25) Levinger, N. E.; Davis, P. H.; Fayer, M. D. *J. Chem. Phys.* **2001**, *115*, 9352.
(26) Gaffney, K.; Piletic, I.; Fayer, M. D. *J. Phys. Chem. A* **2002**, *106*, 9428.
(27) Kuppers, J. R. *J. Electrochem. Soc.* **1978**, *125*, 97.
(28) Gaffney, K. J.; Piletic, I. R.; Fayer, M. D. *J. Chem. Phys.*, accepted
(29) Gaffney, K. J.; Piletic, I. R.; Fayer, M. D. Manuscript in preparation.
(30) Miller, R. E. *Science* **1988**, *240*, 447.
(31) Rey, R.; Hynes, J. T. *J. Chem. Phys.* **1996**, *104*, 2356.
(32) Iwaki, L. K.; Dlott, D. D. *J. Phys. Chem. A* **2000**, *104*, 9101.
(33) Deak, J. C.; Rhea, S. T.; Iwaki, L. K.; Dlott, D. D. *J. Phys. Chem. A* **2000**, *104*, 4866.
(34) Woutersen, S.; Bakker, H. J. *Phys. Rev. Lett.* **1999**, *83*, 2077.
(35) Keutsch, F. N.; Saykally, R. J. *Proc. Natl. Acad. Sci. U.S.A.* **2001**, *98*, 10533.
(36) Keutsch, F. N.; Fellers, R. S.; Brown, M. G.; Viant, M. R.; Petersen, P. B.; Saykally, R. J. *J. Am. Chem. Soc.* **2001**, *123*, 5938.
(37) Berg, M. *J. Phys. Chem. A* **1998**, *102*, 17.
(38) *CRC Handbook of Chemistry and Physics*, 51st ed.; The Chemical Rubber Co.: Cleveland, 1970.
(39) Kindt, J. T.; Schmuttenmaer, C. A. *J. Phys. Chem.* **1996**, *100*, 10373.
(40) Lock, A. J.; Woutersen, S.; Bakker, H. J. *J. Phys. Chem. A* **2001**, *105*, 1238.
(41) Berne, B. J.; Pecora, R. *Dynamic Light Scattering*; J. Wiley: New York, 1976.
(42) Huber, D. L. *Phys. Rev. B* **1979**, *20*, 5333.
(43) Huber, D. L. *Phys. Rev. B* **1979**, *20*, 2307.
(44) Gochanour, C. R.; Andersen, H. C.; Fayer, M. D. *J. Chem. Phys.* **1979**, *70*, 4254.
(45) Gochanour, C. R.; Fayer, M. D. *J. Phys. Chem.* **1981**, *85*, 1989.
(46) Forster, T. *Discuss. Faraday Soc.* **1959**, *27*, 7.
(47) Lipari, G.; Szabo, A. *Biophys. J.* **1980**, *30*, 489.
(48) Wang, C. C.; Pecora, R. *J. Chem. Phys.* **1980**, *72*, 5333.
(49) Barthel, J.; Bachhuber, K.; Buchner, R.; Hetzenauer, H. *Chem. Phys. Lett.* **1990**, *165*, 369.
(50) Petersen, K. A.; Fayer, M. D. *J. Chem. Phys.* **1986**, *85*, 4702.
(51) Woutersen, S.; Bakker, H. J. *Nature (London)* **1999**, *402*, 507.
(52) Tokmakoff, A.; Urdahl, R. S.; Zimdars, D.; Francis, R. S.; Kwok, S.; Fayer, M. D. *J. Chem. Phys.* **1995**, *102*, 3919.
(53) Littau, K. A.; Bai, Y. S.; Fayer, M. D. *Chem. Phys. Lett.* **1989**, *159*, 1.
(54) Littau, K. A.; Dugan, M. A.; Chen, S.; Fayer, M. D. *J. Chem. Phys.* **1992**, *96*, 3484.
(55) Berg, M.; Walsh, C. A.; Narasimhan, L. R.; Littau, K. A.; Fayer, M. D. *J. Chem. Phys.* **1988**, *88*, 1564.
(56) Gale, G. M.; Gallot, G.; Hache, F.; Lascoux, N.; Bratos, S.; Leicknam, J. C. *Phys. Rev. Lett.* **1999**, *82*, 1068.
(57) Palfrey, S. L.; Heinz, T. F. *J. Opt. Soc. Am. B* **1985**, *2*, 674.
(58) Stepanov, B. I. *Nature (London)* **1946**, *157*, 808.